10-12-2010

Doping Dependence of Electronic and Mechanical Properties of $GaSe_{1-x}Te_x$ and $Ga_{1-x}In_xSe$ from First Principles

Zs. Rak

S. D. Mahanti

K. C. Mandal
University of South Carolina - Columbia, mandalk@engr.sc.edu

N. C. Fernelius

Publication Info

Published in *Physical Review B*, Volume 82, Issue 15, 2010, pages 155203-1-155203-10.

Rak, Zs., Mahanti, S. D., Mandal, K. C., & Fernelius, N. C. (12 October 2010). Doping dependence of electronic and mechanical properties of $GaSe_{1-x}Te_x$ and $Ga_{1-x}In_xSe$ from first principles. *Physical Review B*, 82(15), #155203.
http://dx.doi.org/10.1103/PhysRevB.82.155203
http://journals.aps.org/prb/abstract/10.1103/PhysRevB.82.155203

Doping dependence of electronic and mechanical properties of $GaSe_{1-x}Te_x$ and $Ga_{1-x}In_xSe$ from first principles

Zs. Rak,[1,*] S. D. Mahanti,[1] Krishna C. Mandal,[2] and N. C. Fernelius[3]
[1]*Department of Physics and Astronomy, Michigan State University, East Lansing, Michigan 48824, USA*
[2]*Department of Electrical Engineering, University of South Carolina, Columbia, South Carolina 29208, USA*
[3]*AFRL/RX, WPAFB, Dayton, Ohio 45433, USA*

(Received 22 March 2010; revised manuscript received 20 September 2010; published 12 October 2010)

The electronic and mechanical properties of the hexagonal, layered GaSe doped with Te and In have been studied using first-principles pseudopotential method within density-functional theory. The calculated elastic constants of the end compounds GaSe and InSe compare well with the available experimental and theoretical values. As we go from GaSe to InSe, the elastic constants C_{13}, C_{33}, and C_{44} increase while C_{11} and C_{12} decrease, suggesting that the crystal becomes stiffer in the direction perpendicular to the atomic layers and the softer in the direction parallel to the layers, as more substitutional In is incorporated in GaSe. The electronic structure and the formation energies of several defects and simple defect complexes are discussed and the calculated charge transition levels are compared to available experimental data. We demonstrate that In doping may play an important role in the observed enhancement in the structural properties of GaSe. Depending on the Fermi energy, In can either substitute for Ga (In_{Ga}) or occupy an interstitial position as a triply charged defect (In_i^{3+}). While the substitutional In does not change significantly the electronic and mechanical properties of the host, we find that the shear stiffness of GaSe is considerably increased when In is incorporated as charged interstitial impurity.

DOI: 10.1103/PhysRevB.82.155203 PACS number(s): 61.72.Bb, 61.50.Ah, 62.20.de, 71.55.Ht

I. INTRODUCTION

Gallium selenide (GaSe) is an important wide band-gap semiconductor that shows great promise as a nonlinear optical material. Combining a large number attractive properties such as large nonlinear coefficient, high damage threshold, high-temperature operation, wide transparency range,[1–6] GaSe has been investigated for second-harmonic generation, frequency mixing, and generation/detection of terahertz radiation.[7–10] Many of the unique properties of GaSe are associated with its layered crystal structure. One atomic layer consists of two monatomic sheets of Ga sandwiched between two monatomic sheets of Se. The strong covalent interaction within the atomic layers and the week, van der Waals type bonding between the layers render GaSe as a quasi-two-dimensional, highly anisotropic material.

One of the difficulties in the utilization of GaSe crystals in device applications arises from its unsatisfactory mechanical properties regarding cleavability and hardness. It is highly cleavable along planes parallel to the atomic layers and it has almost zero hardness by Mohs scale.[11] Furthermore the nonlinear properties are difficult to reproduce from sample to sample,[7] hampering the use of large-area GaSe crystals in practical applications. It has been observed however, that the structural strength of the GaSe crystals can be improved by incorporating different doping elements in the lattice: In,[11–15] Er,[16] and S.[17,18] Further attempts were made to improve the optical, thermal, and mechanical properties by doping with Ag and mixing with $AgGaSe_2$ to form a solid solution.[14] In the case of In doping, besides the improvement in the mechanical strength of GaSe crystal, enhancement in the nonlinear optical properties has also been reported.[11,12,14,15]

Despite the considerable amount of experimental work, there is a lack of theoretical approach on the subject of the electronic, optical, and mechanical properties of doped GaSe. In this paper, we address this problem by investigating the effect of isovalent doping (Te and In) on the electronic-structure and mechanical characteristics of GaSe. We do this by examining and comparing the mechanical properties of GaSe and InSe, and analyzing the formation energies, charge transition levels, and electronic structure of several point defects and defect complexes associated with Te and In doping. Based on the results of our calculations, we propose an explanation for the experimentally observed rigidity enhancement of GaSe doped with In.

II. METHODS AND COMPUTATIONAL DETAILS

The results presented in this study have been obtained using the projector-augmented wave (PAW) (Refs. 19 and 20) method, within density-functional theory (DFT) (Refs. 21 and 22) as implemented in the Vienna *ab initio* simulation package (VASP).[23–26] The exchange-correlation potential was approximated by the Ceperley-Adler local-density approximation (LDA).[27] The choice of LDA over the generalized gradient approximation (GGA) was motivated by previous theoretical studies on III-VI layered materials, according to which the GGA produces an optimized crystal structure that is excessively elongated in the direction perpendicular to the atomic layers.[28,29] This is because GGA underestimates the week (van de Waals type) bonding between the atomic layers and consequently gives an exceedingly large interlayer separation in comparison to the experiment.

In all our calculations, the outer *s*, *p*, and *d* orbitals of the Ga and In atoms as well as the *s* and *p* orbitals of the Se and Te were included in as valence states while the rest were treated as core states. The cut-off energy for the plane-wave basis was set to 300 eV and the convergence of self-

TABLE I. Strains and elastic moduli for crystals with hexagonal symmetry. ΔE is the change in energy due to the specific strain and V_0 is the equilibrium unit-cell volume.

Strain configuration (unlisted $e_i=0$)	Energy density ($\Delta E/V_0$)
$e_1=e_2=\delta$	$(C_{11}+C_{12})\delta^2$
$e_1=e_2=-2e_3=\delta$	$(C_{11}+C_{12}-4C_{13}+2C_{33})\delta^2$
$e_3=\delta$	$1/2\times(C_{33})\delta^2$
$e_6=\delta$	$1/4\times(C_{11}-C_{12})\delta^2$
$e_4=e_5=\delta$	$(C_{44})\delta^2$

consistent cycles was assumed when the energy difference between them was less than 10^{-4} eV.

To investigate the effect of the isovalent impurities on the physical properties of GaSe, the dopant atoms were placed at several substitutional (Te_{Se}, Te_{Ga}, In_{Ga}) and interstitial (Te_i, In_i) sites inside the host matrix. In addition, we have also examined the electronic structure and defect formation energies associated with substitutional indium-gallium vacancy complex (In_{Ga}-V_{Ga}).

Before discussing the details of electronic-structure and elastic stiffness calculations, we briefly review the method used for the calculation of the elastic constants. The GaSe (and InSe) crystal has hexagonal symmetry therefore it is characterized by five elastic constants: C_{11}, C_{12}, C_{13}, C_{33}, and C_{44}. We have obtained linear combinations of these quantities from total-energy calculations of five different strain configurations. When the lattice is distorted by a small strain, the lattice vectors change according to[30]

$$\mathbf{a}' = (\mathbf{I} + \boldsymbol{\epsilon})\mathbf{a}, \tag{1}$$

where $\mathbf{a}$ and $\mathbf{a}'$ are matrices that contain the components of the old and new lattice vectors, $\mathbf{I}$ is the identity matrix, and $\boldsymbol{\epsilon}$ is the strain matrix, which has the form

$$\boldsymbol{\epsilon} = \begin{bmatrix} e_1 & \frac{1}{2}e_6 & \frac{1}{2}e_5 \\ \frac{1}{2}e_6 & e_2 & \frac{1}{2}e_4 \\ \frac{1}{2}e_5 & \frac{1}{2}e_4 & e_3 \end{bmatrix}. \tag{2}$$

The specific strain configurations along with the corresponding energy densities used to determine the elastic moduli of the hexagonal GaSe and InSe are listed in Table I.

The theoretical crystal structures of $GaSe_{1-x}Te_x$ ($x=0$, 0.0625, 0.25) and $Ga_{1-x}In_xSe$ ($x=0$, 0.0625, 0.25, 1) have been computed by minimizing the total energies with respect to the lattice constants (for each composition x): first with respect to the volume of the unit cell keeping the c/a ratio fixed and then with respect to c/a keeping the previously obtained equilibrium volume fixed. The structures of $GaSe_{1-x}Te_x$ ($x=0$, 0.25) and $Ga_{1-x}In_xSe$ ($x=0$, 0.25, 1) were obtained using small unit cells (8 atoms/cell) where the Brillouin zone (BZ) was sampled by a Γ-centered $12\times12\times3$ k mesh. In the case of $x=0.0625$, the calculations were performed on $2\times2\times1$ supercells with the BZ sampled by a $6\times6\times3$ grid of k points.

The electronic structure and defect formation energies were calculated using $3\times3\times1$ supercells with the theoretical lattice constants of GaSe. The integration of the BZ was carried out on a Γ-centered, $4\times4\times3$ set of k points. The $3\times3\times1$ supercells containing one impurity correspond to a composition with $x\simeq0.028$. In all the calculations, the internal structural parameters were fully relaxed until the Hellmann-Feynman forces were less than 0.02 eV/Å.

The reliability and generality of the image charge correction proposed by Makove and Payne,[31] have been subject of considerable debate in the literature. Since the correction is based on point charge model, its application is only reasonable when the defect-induced perturbation of the charge density is strictly localized around the defect (i.e., only the occupation of localized defect states is changed when electrons are added or removed from the system).[32–34] According to our calculations, the charged defect states associated with In and Te impurities in GaSe are not always localized, for example, as illustrated in Sec. III C 2, In_i introduces a defect level at the top of the valence band (VB) but in neutral charge state, the Fermi level is located above the conduction-band minimum (CBM). When electrons are removed from the system to create a positively charged defect, the occupancy of the delocalized CB states will be affected, making the Makove-Payne (MP) correction meaningless. Similarly, in the case of In_{Ga}-V_{Ga} the calculations show a defect state which is resonant in the CB while the Fermi energy is located below the VB maximum (VBM). Therefore, when electrons are added to the system (up to the charge state $q=2$) they will first occupy the delocalized states ate the top of the VB and bottom of the CB. Based on these considerations, we decided not to include the MP correction in our calculations.

III. RESULTS AND DISCUSSIONS

A. Theoretical crystal structures

The calculated equilibrium lattice parameters of $GaSe_{1-x}Te_x$ and $Ga_{1-x}In_xSe$ are listed in Table II, along with other available theoretical[35,36] and experimental[37] data. In both cases, we observe a monotonic increase in the lattice constants as the concentration of the impurities (x value) increases. This is not surprising because the sizes of the dopant atoms (In and Te) are larger compared to the host atoms. In the case of the end compounds GaSe and InSe, the theoretical lattice constants are ~3% smaller compared to experiment while the c/a ratios are within 0.7% of the experimental values. The underestimation of the lattice parameters is due to the well-known overbinding effect of LDA.

In $GaSe_{1-x}Te_x$, there is a phase transition from hexagonal (GaSe) to monoclinic (GaTe) structure in the composition range $0.26<x<0.60$.[38] Thus, in the case of $GaSe_{1-x}Te_x$, we have limited our calculations to the maximum value of $x=0.25$ because the comparison between the elastic constants and lattice parameters of the monoclinic and hexagonal crystals are not quite meaningful.

TABLE II. Optimized theoretical lattice parameters of $GaSe_{1-x}Te_x$ and $Ga_{1-x}In_xSe$.

Compound	x		a (Å)	c (Å)	c/a	$d_{Ga\text{-}Ga}/c$	$d_{Se\text{-}Se}/c$
	0	Pres. calc.	3.715	15.77	4.244	0.153	0.300
		Theory[a]	3.724	15.68	4.21	0.150	0.350
		Theory[b]	3.720	15.62	4.199	0.154	0.302
$GaSe_{1-x}Te_x$		Experiment[c]	3.755	15.94	4.245		
	0.0625	Te_{Se}	3.733	15.85	4.246		
		Te_i	3.654	17.28	4.730		
	0.25	Te_{Se}	3.801	15.99	4.207		
	0.0625	In_{Ga}	3.730	15.81	4.239		
		In_i	3.800	15.87	4.176		
$Ga_{1-x}In_xSe$	0.25	In_{Ga}	3.773	15.93	4.233		
	1	Pres. Calc.	3.972	16.49	4.151		
		Experiment[c]	4.005	16.64	4.155		

[a]Reference 35.
[b]Reference 36.
[c]Reference 37.

B. Elastic properties

To obtain an intuitive picture about the behavior of the elastic moduli of $Ga_{1-x}In_xSe$ as a function of composition, we have analyzed the elastic properties of the end compounds: GaSe and InSe. In order to determined the elastic constants of GaSe and InSe, we have calculated the total energies of several strained configurations, for δ between −0.03 and 0.03 (see Table I), and fit the results to a second-order polynomial. The calculated values are given in Table III, along with earlier theoretical[35,36] and experimental[39,40] data. The earlier calculations were performed using norm-conserving pseudopotentials and plane-wave (PW) basis sets[35] as well as full-potential augmented plane-wave method with local orbitals.[36] Our calculated values of the elastic moduli of GaSe and InSe using the PAW method are in good agreement with the available experimental values and earlier theoretical calculations.

Comparing the elastic moduli of GaSe and InSe, we observe a decrease in C_{11} and C_{12} and an increase in C_{13}, C_{33}, and C_{44}. Assuming a monotonic behavior for the elastic constants of $Ga_{1-x}In_xSe$ as a function of composition (x value), this indicates that when the concentration substitutional In increases, the crystal becomes softer in the a and b directions (parallel to the atomic layers) and stiffer along the c axis (perpendicular to the atomic layers).

This, apparently peculiar behavior of the elastic constants of $Ga_{1-x}In_xSe$, can be explained after a careful analysis of the connection between the structural and electronic properties of the end compounds: GaSe and InSe. Although the electronic structure of the III-VI layered compounds have been discussed in details in several earlier reports (e.g., Ref. 29), we have recalculated their band structures (Fig. 1), for a direct comparison. First let us analyze the top of the VB, which is mainly of Se p_z character. Since the elasticity of the layered $Ga_{1-x}In_xSe$ in the c direction is determined predominantly by the interaction between the atomic layers, and the Se p_z orbitals are the ones facing the interlayer region, we expect that the dispersion of the top VB along the Γ-A direction to be sensitive to the interlayer interaction. Indeed,

TABLE III. Elastic constants of $Ga_{1-x}In_xSe$ (x=0,1). All values are given in gigapascal.

x		C_{11}	C_{12}	C_{13}	C_{33}	C_{44}	$C_{11}+C_{12}$	$C_{11}-C_{12}$
0	Pres. calc.	100.9	27.0	9.7	33.9	8.3	127.9	73.8
	Theory[a]			12.4	35.4		130.2	
	Theory[b]			13.4	34.4		127.9	
	Experiment[c]			12.2	35.7		132.5	
	Experiment[d]	105.0	32.4	12.6	35.1	10.4	137.4	72.6
1	Pres. calc.	70.3	23.5	14.2	38.5	11.5	93.9	46.9
	Experiment[d]	73.0	27.0		36.0		100.0	46.0

[a]Reference 35.
[b]Reference 36.
[c]Reference 39.
[d]Reference 40.

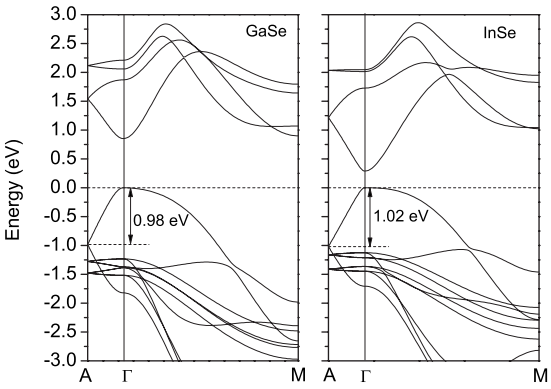

FIG. 1. The calculated band structures of GaSe and InSe. A-Γ and Γ-M directions are perpendicular and parallel to the atomic layers, respectively.

according to our calculated band structure, the Γ-A dispersion of the top VB increases by ~40 meV (see Fig. 1) in going from GaSe to InSe, indicating that the interlayer interaction is stronger in InSe compared to GaSe. This is consistent with the smaller interlayer separation in InSe (2.96 Å) than in GaSe (3.15 Å). Thus, when the concentration of In substitutional impurities increases, the interlayer Se-Se distance becomes smaller, the interaction becomes stronger, and as a consequence, the crystal becomes stiffer in the direction perpendicular to the atomic layers.

The softening of $Ga_{1-x}In_xSe$ in the *a* and *b* directions with the increase in the composition *x* can also be easily understood because the intralayer distances are longer and therefore the intralayer covalent bonds are weaker in InSe than in GaSe.[41,42] Inspecting Fig. 1 we observe that indeed, the lower-lying valence bands of InSe, with predominantly Se p_x and Se p_y character, disperse less in the Γ-M direction compared to the corresponding bands of the GaSe. Since in the *a* and *b* directions there is no "interlayer region" which could counteract the weakening of the atomic bonds, the crystal becomes softer with the increase in the In concentration.

Although the substitutional In impurity seems to enhance the elastic properties of GaSe along the *c* axis, the effect is rather small (e.g., C_{33} increases by only 7.8% from GaSe to InSe). Therefore, we have to look for different mechanisms to explain the In-induced interlayer rigidity enhancement as seen experimentally.[11,12,14,15] Before discussing this aspect (in Sec. III D), we describe the formation energies of different defects to find out which defect is more likely to be present in GaSe.

C. Formation energies and electronic structure of defects

In order to identify the most stable locations for the impurities inside the GaSe matrix, we have calculated the formation energies of substitutional and interstitial Te and In impurities in several different configurations. For this we have applied the formalism described by Zhang *et al.*,[43,44] according to which the formation energy of a defect *D* in a charge state *q*, denoted as D^q, is given by

$$\Delta H_f(D^q) = \Delta E(D^q) + \sum_i (n_i \mu_i) + qE_F, \quad (3)$$

$$\Delta E(D^q) = E(D^q) - E(\mathrm{GaSe}) + \sum_i [n_i E(i)] + qE_{\mathrm{VBM}}. \quad (4)$$

In Eqs. (3) and (4), $E(D^q)$ and E(GaSe) are the total energies of the defect-containing and the defect-free supercells and $E(i)$'s (i=Ga, Se, In, and Te) are the energies of the constituents in their standard solid state. The atomic chemical potentials μ_i's are referenced to the corresponding $E(i)$'s and n_i's are the number of atoms removed from ($n_i>0$) or added to ($n_i<0$) the system. In supercell calculations, the VBM is usually considered to be the reference for the electron chemical potential (Fermi energy, E_F). In the present study, the energy of the VBM (E_{VBM}) was determined as the average one-electron energy level of the highest VB over the *k* points where the total energy was calculated. This approach has the advantage that charge transition levels calculated this way [see Eq. (5) below] are consistent with the single-particle energy levels.[44] Furthermore, in the present case, the "average band-edge" method shifts VBM and CBM by −0.45 eV and 0.35 eV, respectively, producing a semiconducting band gap ($E_{\mathrm{gap}}^{\mathrm{average}}$=1.68 eV) which is closer to the experimental value ($E_{\mathrm{gap}}^{\mathrm{exp}}$=2.13 eV) than the direct gap calculated at the Γ point ($E_{\mathrm{gap}}^{\Gamma}$=0.85 eV). We would like to point out that the average band-edge approach used in our calculations is not a band-gap correction method, and changes in the *k*-point sampling can lead to slightly different results.

In order to check the accuracy of our calculations in comparison to experiment, we have also calculated the charge transition levels, denoted as $\epsilon(q/q')$, which correspond to the values of E_F where the formation energies of a defect in two different charge states (q and q') are equal,[43,44]

$$\epsilon(q/q') = [\Delta E(D^{q'}) - \Delta E(D^q)]/(q - q'). \quad (5)$$

According to Eqs. (3) and (4), the formation energy of a defect depends on the chemical potentials of the constituents (μ) as well as on the charge state (q) of the particular defect. The values achievable by the chemical potentials are limited by several equilibrium growth conditions (see, for example, Refs. 44 and 45): (a) to avoid precipitations, μ_i's must be negative and (b) to maintain a stable host compound, the chemical potential must satisfy $\mu_{\mathrm{Ga}}+\mu_{\mathrm{Se}}=\Delta H$(GaSe), where ΔH(GaSe) is the formation enthalpy of GaSe. Our theoretical calculation gives ΔH(GaSe)=−1.12 eV so the Se-rich or Ga-rich growth conditions can be simulated by adjusting the chemical potentials μ_{Se} or μ_{Ga} between −1.12 and 0 eV. (c) In order to avoid the formation of secondary phases between the host elements and impurities, several further conditions have to be imposed on the chemical potentials: $\mu_{\mathrm{In}}+\mu_{\mathrm{Se}} \leq \Delta H$(InSe) and $\mu_{\mathrm{Te}}+\mu_{\mathrm{Ga}} \leq \Delta H$(GaTe), where ΔH(InSe)=−0.95 eV and ΔH(GaTe)=−0.64 eV are the calculated formation enthalpies of InSe and GaTe, respectively.

In Fig. 2, the calculated Te and In defect formation energies are shown, under Ga-rich (μ_{Ga}=0; μ_{Se}=−1.12 eV) and Se-rich (μ_{Ga}=−1.12 eV; μ_{Se}=0) growth conditions. In these figures, both the theoretical ($E_{\mathrm{gap}}^{\mathrm{theor}}$=1.68 eV) and experimental ($E_{\mathrm{gap}}^{\mathrm{exp}}$=2.13 eV) band gaps are indicated. The calculated defect transition levels $\varepsilon(q/q')$ and formation energies $\Delta E(X^q, q=0)$ are listed in Table IV.

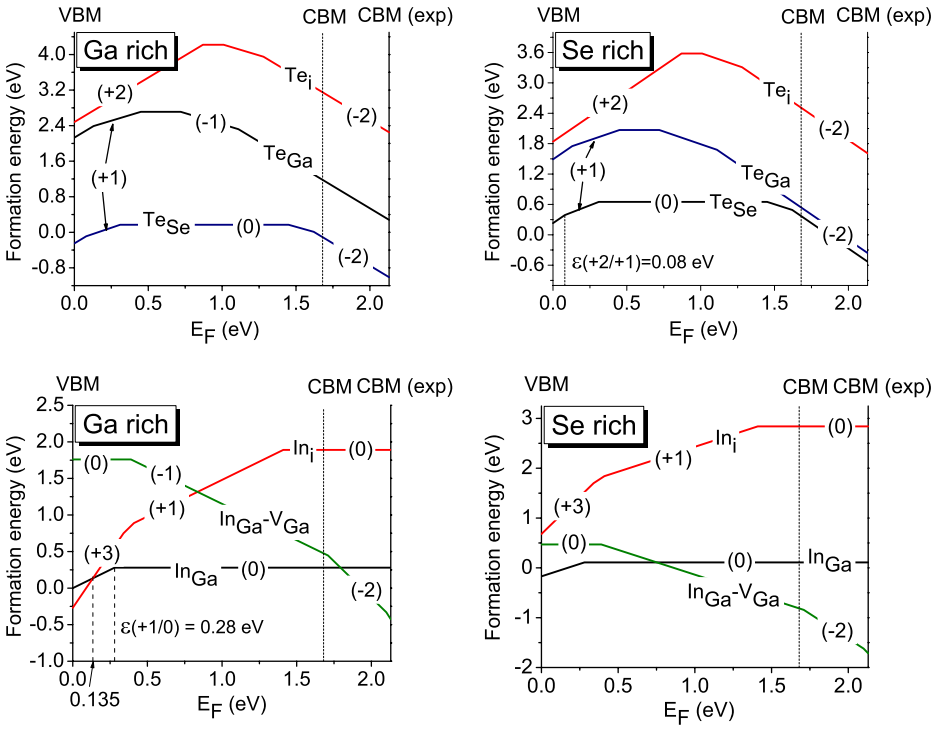

FIG. 2. (Color online) (a) and (b) Formation energies of Te impurity in GaSe under Ga-rich and Se-rich conditions, respectively. For all values of E_F within the band gap, Te prefers to occupy the Se site. (c) Formation energies of In impurity in GaSe under Ga-rich conditions. When E_F is very close to VBM, the In impurity becomes positively charged (+3) and moves to the interstitial site. (d) Formation energies of In-related defects in GaSe under Se-rich conditions.

1. Te-induced defects

In the case of Te doping, we have considered the configurations with Te located at Se and Ga sites as well as at the interstitial site. The interstitial configuration with the lowest energy was found when the impurity atom was located midway between the Ga-Se-Se-Ga layers at equal distances from the six nearest-neighbor (NN) Se atoms.

The formation energies of the Te-induced defects, under Ga-rich ($\mu_{Ga}=0$, $\mu_{Se}=-1.12$ eV) and Se-rich ($\mu_{Ga}=-1.12$ eV, $\mu_{Se}=0$) growth condition are shown in Figs. 2(a) and 2(b), respectively. In both cases, the lowest formation energy occurs when the Te atom is located at a Se site (Te_{Se}). In neutral charge state, under Ga-rich condition, the calculated formation energy of Te_{Se} is $\Delta H_f(Te^0_{Se})=0.17$ eV. Under Se-rich condition, this value increases to $\Delta H_f(Te^0_{Se})=0.65$ eV, as there are less Se vacancies that could accommodate the Te impurities. If the Fermi energy (E_F) is tuned closer to the VB (p-type sample), Te_{Se} becomes positively charged, and gives rise to two charge transition levels located at $\varepsilon(+2/+1)=0.08$ eV and $\varepsilon(+1/0)=0.31$ eV above the VBM. Photoluminescence and Hall effect measurements have shown that the carrier transport in p-GaSe doped with Te, is dominated by two acceptor levels at 0.08 and 0.02 eV above the VB.[46,47] Our calculated $\varepsilon(+2/+1)$ transition level is in excellent agreement one of the experimental values. When the Fermi energy (E_F) is close to the CB (n-type conductivity), Te_{Se} becomes negatively charged, the transition levels being located at $\varepsilon(0/-1)=1.45$ eV and $\varepsilon(-1/-2)=1.62$ eV above the VBM.

The formation energy of the substitutional Te atom at the Ga site (Te_{Ga}) is slightly higher compared to Te_{Se}. However, under Se-rich condition, and when the defect is in −2 charge state (Te^{-2}_{Ga}), the difference between the formation energies $\Delta H_f(Te^{-2}_{Se})$ and $\Delta H_f(Te^{-2}_{Ga})$ becomes quite small (~0.18 eV) suggesting that Te atoms can fill up the Ga vacancies. However, under Ga-rich condition, according to Eqs. (3) and (4), and taking into account the equilibrium growth conditions described in Sec. III C, the formation energy of Te_{Ga} is shifted up by 0.64 eV, making it less likely

TABLE IV. Formation energies of neutral defects and the charge transition levels. All values are given in electron volt.

		Transition levels (measured from the VBM)					
Defect	$\Delta E(X^0)$	$\varepsilon(+3/+2)$	$\varepsilon(+2/+1)$	$\varepsilon(+1/0)$	$\varepsilon(0/-1)$	$\varepsilon(-1/-2)$	$\varepsilon(-2/-3)$
Te_{Se}	0.65		0.08	0.34	1.45	1.62	
Te_{Ga}	2.07		0.13	0.45	0.72	1.11	
Te_i	3.58		1.04	0.70	1.01	1.28	
In_{Ga}	0.28	−0.10	−0.02	0.28			
In_i	1.89	0.34	0.41	1.41			
In_{Ga}-V_{Ga}	1.76				0.39	1.71	2.10

for Te to occupy Ga site. This is because under Ga-rich condition ($\mu_{Ga}=0$), the chemical potential of the Te is limited by $\mu_{Te} \leq -0.64$ eV, in order to avoid the formation of GaTe as a secondary phase.

The interstitial Te defect (Te_i) has the highest formation energy and therefore it is less likely to occur. As shown in Fig. 2(a), the formation energy of this defect in neutral charge state $\Delta H_f(Te_i^0)$ is almost 4 eV higher compared to $\Delta H_f(Te_{Se}^0)$, and the difference becomes somewhat smaller when Te_i is in doubly charged negative (Te_i^{-2}) or positive (Te_i^{+2}) state. However, according to recent experimental results of Evtodiev *et al.*[47] at high Te doping concentration, some of the Te atoms localize in the interstitial sites within the interlayer region. Therefore we cannot exclude the possibility that the Te atoms can occupy interstitial sites, which clearly would affect the cleavability of the GaSe crystal. It is also interesting to note that the Te related defects can behave as either donor or acceptor, depending on the position of E_F relative to the band edges.

2. In-induced defects

Three types of In related defects have been investigated: In substituting for Ga (In_{Ga}), interstitial In (In_i), and substitutional In-Ga vacancy complex (In_{Ga}-V_{Ga}). The calculated formation energies under Ga- and Se-rich condition are shown in Figs. 2(c) and 2(d). We observe that In_{Ga} introduces a charge transition level $\epsilon(+1/0)=0.28$ eV above the VB, which is in reasonably good agreement with the acceptor level at 0.21 eV reported by Cui *et al.*[48] Moreover, the calculated transition level $\epsilon(+2/+1)=0.41$ eV, associated with In_i, is quite close to the acceptor level located at 0.46 eV above the VB, measured by Shigetomi and Ikari in In-doped GaSe.[49] They have associated this acceptor level with the complex center of In interstitial and Se vacancy. These calculated values, along with the charge transition levels obtained for Te_{Se}, discussed in the previous section, suggest that our total-energy calculations based on supercell models are adequate for a quantitative description of the defect physics in GaSe.

Under Ga-rich growth condition, the defects with the lowest formation energies are: In_i^{3+} for $E_{VBM}(=0 \text{ eV}) \leq E_F \leq 0.135$ eV, In_{Ga}^{1+} for $0.135 \leq E_F \leq 0.28$ eV, and In_{Ga}^0 for $0.28 \text{ eV} \leq E_F$. The most stable defect for a wide range of E_F is In_{Ga}^0. However, according to our calculations, when the Fermi energy is tuned toward the VBM (p-type GaSe), In_i^{3+} becomes the more stable compared to In_{Ga} [see Fig. 2(c)]. At this point, we would like to emphasize that the calculated stability range of In_i^{3+} is quite narrow (~0.14 eV) and it was obtained using the average band-edge method described in Sec. III C, where the VBM is determined as the average over the k points. Therefore, the calculated VBM is shifted by down in energy by 0.45 eV compared to the VBM at the Γ point and as a result our calculated stability range of In_i^{3+} might appear slightly overestimated. If the VBM at the Γ point were used in the calculations, the stable energy range would be narrower (or could even vanish). Later we will discuss the underlying physics and the stability of In_i^{3+} defect by analyzing its electronic structure.

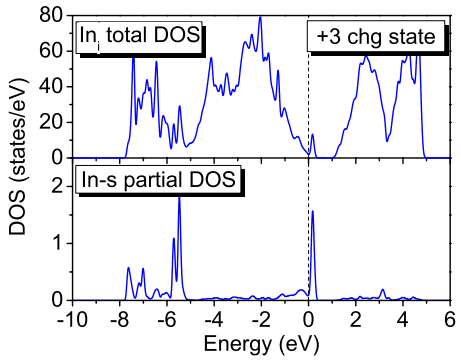

FIG. 3. (Color online) The total DOS of GaSe with In_i and the projected DOS of the In s orbital, showing the positions of the HDDS (−5.5 eV) and DDS (just above E_F) introduced by the charged In_i defect.

Regarding the effect of In_{Ga}^0 on the electronic structure of GaSe, we find that the band structure near VBM and CBM are affected very little. One therefore does not expect much change in the transport properties in In-doped GaSe if the impurity goes to a Ga site in the neutral charge state. This lack of significant change can be explained by looking at the In 5s-Ga 4s dimer antibonding state (which hybridizes with the Se p bands to give rise to states in the neighborhood of the band gap) and observe that it is not significantly different from the Ga 4s-Ga 4s dimer antibonding state.[29]

The stability of In_i^{3+} defect, when $E_F \leq 0.135$ eV, can be understood if we analyze the electronic structure, the single-particle (DOS) and the nature of defect state introduced by In_i. Figure 3 shows the total DOS as well as the In s partial DOS for this case. We observe that In_i introduces a defect state near the bottom of the Se p bands (at ~−5.5 eV), which we call hyper deep defect state (HDDS). This is a bonding state formed out of In 5s and neighboring Se p orbitals. The corresponding antibonding combination located at the top of the VBM, splits off from the Se p valence-band states and is denoted as the DDS. The localized nature of the DDS is evident from the charge-density distribution represented in Fig. 4, which also shows that the DDS is indeed an antibonding combination of the In s and the surrounding Se p orbitals. This physical picture of the In_i-induced defect

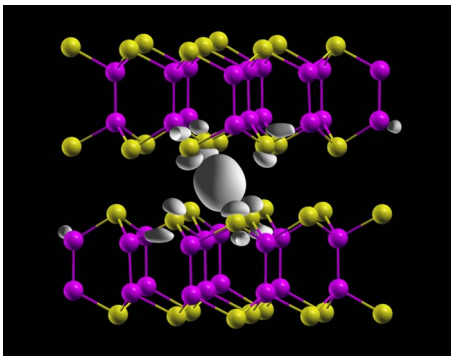

FIG. 4. (Color online) Charge-density distribution associated with the localized band introduced by In_i in the band gap of GaSe. The dominant contribution comes from the In s orbital, hybridized with the NN Se p_z orbitals.

state on GaSe is similar to the case of substitutional In defect in PbTe.[50,51] The strong mixing between In 5*s* and the neighboring Se *p* states leads to the removal of one state (per spin) from the Se *p* band which becomes the DDS. The electron counting is such that, two of the three electrons from In occupy the HDDS while the remaining electron of In together with two other electrons occupying the VB of pure GaSe fill up the DDS and partially occupy the bottom of the CB. Therefore In_i acts like a donor. Since the three electrons occupy states with energies higher than E_{VBM}, clearly the formation energy of In_i in charge state $q=0$, 1, and 2 are higher than In_{Ga} for which neither the band structure nor the electron count change. However, by removing three electrons from In_i, to obtain $q=3$ charge state, we can lower its formation energy.[52] Despite the narrow stability range of In_i^{3+} ($E_F<0.135$ eV), it has been found experimentally that in *p*-GaSe, In can occupy interstitial sites, where the extra electrons associated with In_i^{3+} can be accommodated by holes coming from some other defects.[49] The effect of the In_i^{3+} defect on the mechanical properties of the GaSe crystal will be discussed later, in Sec. III D

Under Se-rich growth condition [Fig. 2(d)], In_i^{3+} becomes thermodynamically unstable. This is because in order to avoid the formation of stable InSe phase under Se-rich condition ($\mu_{Se}=0$), the highest possible value for μ_{In} is −0.95 eV. Therefore, according to Eq. (3), the formation energy of In_i is shifted up by 0.95 eV, making it less likely for the defect to appear. This makes sense because under Se-rich condition, the In atoms can easily accommodated by the increased number of Ga vacancies.

Figures 2(c) and 2(d) also show the calculated defect formation energies associated with the substitutional In-Ga vacancy complex (In_{Ga}-V_{Ga}). Under Ga-rich condition [Fig. 2(c)], the formation energy of this defect complex in neutral charge state is relatively high. However, as the position of the E_F moves up in energy across the band gap, In_{Ga}-V_{Ga} becomes negatively charged and its formation energy decreases considerably, giving rise to a small stability range within the experimental band gap. Under Se-rich condition [Fig. 2(d)] the stability range increases even further and the defect complex becomes stable within more than half of the theoretical band gap, for $E_F>0.75$ eV. We find one transition level associated with this defect complex, located at $\varepsilon(0/-1)=0.40$ eV, which is in good agreement with the acceptor level at 0.44 eV, measured using deep level transient spectroscopy and assigned to In_{Ga}-V_{Ga}, by Cui *et al.*[48] As shown in Figs. 2(c) and 2(d), the other two calculated transition levels of In_{Ga}-V_{Ga} are located above the theoretical CBM but within the experimental gap. The values are also listed in Table IV.

To obtain a better understanding of the nature of the defect states introduced by In_{Ga}-V_{Ga}, we calculated the total DOS associated with this defect complex in different charge states. As shown in Fig. 5, the DOS shows an interesting feature which is only present for the −3 charge state: a localized level appears in the gap (indicated by the arrow in Fig. 5). The origin of this defect state can be understood from a careful analysis of the relationship between the ionic relaxation and the bonding of In and its NN Se atoms. From the charge-density distribution shown in Fig. 6, we see that

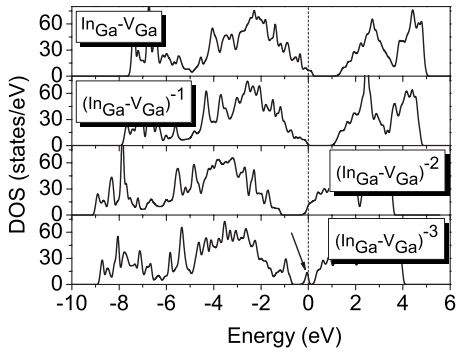

FIG. 5. The total density of states associated with In_{Ga}-V_{Ga} defect complex, for different charge states. When the defect complex is triply negatively charged, the defect state is located in the gap (lower panel).

the defect state in fact corresponds to the antibonding combination of In *s* and its NN Se p_z orbitals, with the dominant contribution coming from the In *s* orbital. To locate the corresponding bonding combination, we have calculated the partial density of states associated with the In *s* orbital. This is represented in Fig. 8 where we have plotted the In *s* partial DOS corresponding to the neutral and −3 charge states of In_{Ga}-V_{Ga}. The origin of the energy scale was chosen at the highest occupied energy state. We notice that the splitting between the bonding and antibonding levels decrease by ~1.5 eV as the defect complex becomes triply negatively charged. To pin down the cause of this energy shift, we have examined the differences between the ionic relaxations of neutral and triply charged systems. We find that independently of the charge state, the In atom prefers to occupy the position located at the center of the Ga-Se-Se-Ga atomic layer, at equal distances from the six NN Se atoms (see Fig. 6). However, as more negative charge is localized at the defect center, the Coulomb attraction between the In ion and the neighboring Se anions becomes weaker and therefore the distances between In and its NN Se atoms increase. We find that the average In-Se distance increases by ~0.34 Å as the state of the defect center changes from neutral to the triply negatively charged. The splitting between the In *s*-Se p_z bonding and antibonding states becomes smaller as the sepa-

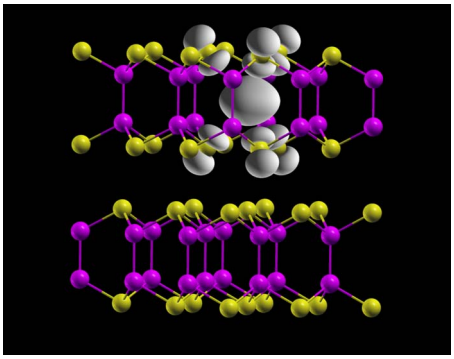

FIG. 6. (Color online) Charge-density distribution associated with the localized band introduced by In_{Ga}-V_{Ga} in the band gap of GaSe. The dominant contribution comes from the In *s* orbital, hybridized with the NN Se p_z orbitals.

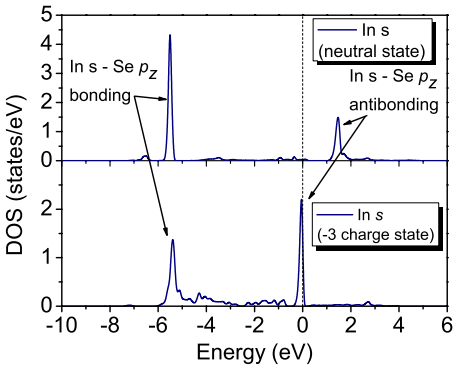

FIG. 7. (Color online) The DOS projected on the In *s* orbital for the neutral and −3 charge state of the In_{Ga}-V_{Ga} defect complex. The splitting between the bonding and antibonding states decreases mainly because the distance between the In and Se atoms increases.

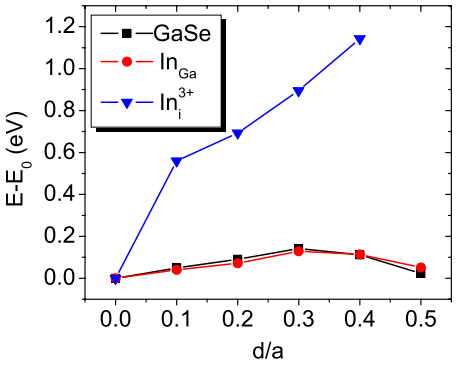

FIG. 8. (Color online) The energy barrier which must be overcome in order to cleave the GaSe crystal increases dramatically when In occupies the interstitial site compared to the case when In occupies substitutional site. For comparison the case of pure GaSe is also shown.

ration between the atoms becomes larger. Consequently, at −3 charge state (when the In-Se distance is the largest), the energy of the antibonding state becomes small enough such that it appears to be located in the band gap of GaSe (Fig. 7). For all the other charge states, the In *s*-Se p_z antibonding combination is resonant with the CB. However, because of the well-known band-gap problem of DFT-LDA, it is not clear whether this defect state is localized in the band gap or its position depends on the energy level of the CBM. Further investigations are required to clarify this issue.

D. Rigidity enhancement of GaSe by In doping

In this section, we discuss the mechanism responsible for rigidity enhancement of the GaSe crystal doped with In. The model described here is quite general and applicable to a large class of layered materials with weak interlayer bonding.

As we have seen in Sec. III B, the elastic properties do not change appreciably in In-doped GaSe when In goes as a substitutional impurity. To further investigate the effect of substitutional In on the mechanical properties of GaSe, we have calculated the energy barrier associated with the relative shearing of two atomic layers in a supercell (each layer being made up from four-monatomic sheets). This is shown in Fig. 8 when the atomic layers are displaced by 0.5*a* relative to each other (*a* is lattice constant of GaSe). We observe that the energy barriers for both pure GaSe and $Ga_{1-x}In_xSe$ are very small and comparable and they follow similar trends as the atomic layers are displaced gradually from 0.1*a* to 0.5*a*. Thus substitutional In does not appear to enhance the shear rigidity of GaSe. Figure 8 also shows the energy barrier associated with similar shearing in the presence of an interstitial charged In defect (In_i^{3+}). This configuration appears to be quite different from the previous two cases: in the presence of In_i^{3+}, the energy barrier and its initial slope increase dramatically (by factors of ~8 and ~11, respectively). This indicates that the soft and cleavable GaSe crystal becomes quite rigid against shear distortion when charged In defects are inserted in the interlayer region. However, we note that this charge state of In_i is stable only when the Fermi energy is closer to the VBM, most likely in *p*-doped systems.

E. Impurity clustering

We have also investigated the possibility of In and Te cluster formation inside the GaSe host. This was done by performing supercell ($3\times3\times1$, 72 atoms) calculations with impurities located close and far away from each other and comparing the corresponding total energies. These calculations were performed using the theoretical lattice constants of GaSe and relaxing all the internal atomic positions. In the case of pure Te doping, we find that the total energy is 40 meV/supercell lower when the impurities are located far from each other, suggesting that Te clustering does not take place. In the case of pure In doping, the situation is similar but the energy difference is smaller: 9 meV/supercell. Considering that the accuracy of our total energy calculations is less than 10 meV, we cannot exclude the possibility of In clustering in GaSe.

IV. SUMMARY

Using first-principles methods within DFT have investigated the elastic properties of $Ga_{1-x}In_xSe$, based on the results obtained for the end compounds GaSe and InSe and assuming a monotonic behavior for of the elastic constants as a function of defect concentration. In the case of substitutional In doping (In_{Ga}), we find that the C_{13}, C_{33}, and C_{44} increase while C_{11} and C_{12} decrease as we go from GaSe to InSe. This indicates a strengthening of the crystal in along the *c* direction (perpendicular to the atomic layers) and a softening in the *a* and *b* directions (parallel to the atomic layers). However, the increase in the elastic stiffness in the *c* direction is very small and cannot explain the experimentally observed improvement in the mechanical properties of In-doped GaSe.

We find that in the case of In_{Ga}-V_{Ga} defect complex, the atomic relaxation plays a major role in the stabilization of the charge states. The variations in the distance between the host Se atoms and the In impurity as a function of the charge states, are responsible for the position of the defect level relative to the band edges of GaSe. One should be able to probe this defect using experimental methods.

The defect formation energy calculations show that Te and In prefer the substitutional Se and Ga sites, respectively. Nevertheless, in the case *p*-type GaSe (when E_F is close to VBM) indium impurity can acquire +3 charge state and occupy interstitial sites between the GaSe layers. This strongly influences the cleavability of the crystal along planes parallel to the atomic layers. We suggest that these defects are most likely the source of the observed improvement of the structural properties of In-doped GaSe.[11,12,14,15]

ACKNOWLEDGMENTS

One of the authors (K.C.M.) acknowledges financial support by the Air Force under Contract No. FA 86540-06-M-541. This work made use of the High Performance Computing Center at Michigan State University.

*Present address: Department of Geological Sciences, University of Michigan, Ann Arbor, MI 48109, USA; rakzsolt@umich.edu

[1] C. Manfredotti, R. Murri, and L. Vasanelli, Nucl. Instrum. Methods **115**, 349 (1974).
[2] A. M. Mancini, C. Manfredotti, R. Murri, A. Rizzo, A. Quirini, and L. Vasanelli, IEEE Trans. Nucl. Sci. **23**, 189 (1976).
[3] E. Sakai, H. Nakatani, C. Tatsuyama, and F. Takeda, IEEE Trans. Nucl. Sci. **35**, 85 (1988).
[4] H. Nakatani, E. Sakai, C. Tatsuyama, and F. Takeda, Nucl. Instrum. Methods **283**, 303 (1989).
[5] T. Yamazaki, H. Nakatani, and N. Ikeda, Jpn. J. Appl. Phys. **32**, 1857 (1993).
[6] T. Yamazaki, K. Terayama, T. Shimazaki, and H. Nakatani, Jpn. J. Appl. Phys. **36**, 378 (1997).
[7] N. C. Fernelius, Prog. Cryst. Growth Charact. Mater. **28**, 275 (1994).
[8] V. G. Dimitriev, G. G. Gurzadyhan, and D. N. Nikogosyan, *Handbook of Nonlinear Optical Crystals* (Springer, New York, 1999).
[9] K. Liu, J. Z. Xu, and X. C. Zhang, Appl. Phys. Lett. **85**, 863 (2004).
[10] K. Liu, J. Xu, and X.-C. Zhang, Proceedings of the Joint 29th International Conference on Infrared and Millimeter Waves and 12th International Conference on Terahertz Electronics, 2004, p. 333.
[11] Z. S. Feng, Z. H. Kang, F. G. Wu, J. Y. Gao, Y. Jiang, H. Z. Zhang, Y. M. Andreev, G. V. Lanskii, V. V. Atuchin, and T. A. Gavrilova, Opt. Express **16**, 9978 (2008).
[12] D. R. Suhre, N. B. Singh, V. Balakrishna, N. C. Fernelius, and F. K. Hopkins, Opt. Lett. **22**, 775 (1997).
[13] N. B. Singh, D. R. Suhre, V. Balakrishna, M. Marable, R. Meyer, N. Fernelius, F. K. Hopkins, and D. Zelmon, Prog. Cryst. Growth Charact. Mater. **37**, 47 (1998).
[14] N. B. Singh, D. R. Suhre, W. Rosch, R. Meyer, M. Marable, N. C. Fernelius, F. K. Hopkins, D. E. Zelmon, and R. Narayanan, J. Cryst. Growth **198-199**, 588 (1999).
[15] V. G. Voevodin, O. V. Voevodina, S. A. Bereznaya, Z. V. Korotchenko, A. N. Morozov, S. Y. Sarkisov, N. C. Fernelius, and J. T. Goldstein, Opt. Mater. **26**, 495 (2004).
[16] C.-W. Chen, Y.-K. Hsu, J. Y. Huang, and C.-C. Chang, Opt. Express **14**, 10636 (2006).
[17] S. Das, G. Ghosh, O. G. Voevodina, Y. M. Andreev, and S. Y. Sarkisov, Appl. Phys. B: Lasers Opt. **82**, 43 (2006).
[18] Yu. M. Andreev, V. V. Atuchin, G. V. Lanskii, A. N. Morozov, L. D. Pokrovsky, S. Yu. Sarkisov, and O. V. Voevodina, Mater. Sci. Eng., B **128**, 205 (2006).
[19] P. E. Blöchl, Phys. Rev. B **50**, 17953 (1994).
[20] G. Kresse and D. Joubert, Phys. Rev. B **59**, 1758 (1999).
[21] P. Hohenberg and W. Kohn, Phys. Rev. B **136**, B864 (1964).
[22] W. Kohn and L. J. Sham, Phys. Rev. **140**, A1133 (1965).
[23] G. Kresse and J. Hafner, Phys. Rev. B **47**, 558 (1993).
[24] G. Kresse and J. Hafner, Phys. Rev. B **49**, 14251 (1994).
[25] G. Kresse and J. Furthmuller, Phys. Rev. B **54**, 11169 (1996).
[26] G. Kresse and J. Furthmuller, Comput. Mater. Sci. **6**, 15 (1996).
[27] D. M. Ceperley and B. J. Alder, Phys. Rev. Lett. **45**, 566 (1980).
[28] Zs. Rak, S. D. Mahanti, K. C. Mandal, and N. C. Fernelius, J. Phys.: Condens. Matter **21**, 015504 (2009).
[29] Zs. Rak, S. D. Mahanti, K. C. Mandal, and N. C. Fernelius, J. Phys. Chem. Solids **70**, 344 (2009).
[30] M. J. Mehl, Phys. Rev. B **47**, 2493 (1993).
[31] G. Makov and M. C. Payne, Phys. Rev. B **51**, 4014 (1995).
[32] D. Segev and S.-H. Wei, Phys. Rev. Lett. **91**, 126406 (2003).
[33] C. G. Van de Walle and J. Neugebauer, J. Appl. Phys. **95**, 3851 (2004).
[34] J. Shim, E.-K. Lee, Y. J. Lee, and R. M. Nieminen, Phys. Rev. B **71**, 035206 (2005).
[35] C. Adler, R. Honke, P. Pavone, and U. Schroder, Phys. Rev. B **57**, 3726 (1998).
[36] D.-W. Zhang, F.-T. Jin, and J.-M. Yuan, Chin. Phys. Lett. **23**, 1876 (2006).
[37] O. Madelung, *Semiconductors: Data Handbook*, 3rd ed. (Springer, Berlin, 2004).
[38] F. Cerdeira, E. A. Meneses, and A. Gouskov, Phys. Rev. B **16**, 1648 (1977).
[39] O. Madelung, *Semiconductors: Physics of Non-Tetrahedrally Bonded Binary Compounds II* (Springer-Verlag, Berlin, 1983), Vol. 17.
[40] M. Gatulle, M. Fischer, and A. Chevy, Phys. Status Solidi B **119**, 327 (1983).
[41] D. Errandonea, A. Segura, F. J. Manjon, A. Chevy, E. Machado, G. Tobias, P. Ordejon, and E. Canadell, Phys. Rev. B **71**, 125206 (2005).
[42] M. O. D. Camara, A. Mauger, and I. Devos, Phys. Rev. B **65**, 205308 (2002).
[43] S. B. Zhang and J. E. Northrup, Phys. Rev. Lett. **67**, 2339 (1991).
[44] S. B. Zhang, J. Phys.: Condens. Matter **14**, R881 (2002).
[45] S. H. Wei and S. B. Zhang, Phys. Rev. B **66**, 155211 (2002).
[46] S. Shigetomi and T. Ikari, J. Appl. Phys. **95**, 6480 (2004).
[47] I. Evtodiev, L. Leontie, M. Caraman, M. Stamate, and E. Arama, J. Appl. Phys. **105**, 023524 (2009).
[48] Y. L. Cui, R. Dupere, A. Burger, D. Johnstone, K. C. Mandal, and S. A. Payne, J. Appl. Phys. **103**, 013710 (2008).

[49] S. Shigetomi and T. Ikari, Jpn. J. Appl. Phys. **46**, 5774 (2007).
[50] S. Ahmad, K. Hoang, and S. D. Mahanti, Phys. Rev. Lett. **96**, 056403 (2006).
[51] K. Hoang and S. D. Mahanti, Phys. Rev. B **78**, 085111 (2008).
[52] The formation energy of neutral In interstitial defect is underestimated in our calculation since one electron/defect occupies the bottom of the conduction band instead of the defect state (which is resonant in the CB), and the LDA gap is 0.85 eV compared to the average band gap of 1.68 eV and the experimental value of 2.13 eV.